Acta Pharmaceutica Sinica B 2021;11(12):3779–3790

Chinese Pharmaceutical Association
Institute of Materia Medica, Chinese Academy of Medical Sciences

Acta Pharmaceutica Sinica B

www.elsevier.com/locate/apsb
www.sciencedirect.com

ORIGINAL ARTICLE

Mechanistic studies of PEG-asparaginase-induced liver injury and hepatic steatosis in mice

Gundala Venkata Naveen Kumar[a,†], Keito Hoshitsuki[a,b,†], Sanjay Rathod[a], Manda J. Ramsey[a], Lauren Kokai[c], Erin E. Kershaw[d], Wen Xie[a], Christian A. Fernandez[a,*]

[a]*Department of Pharmaceutical Sciences and Center for Pharmacogenetics, University of Pittsburgh School of Pharmacy, Pittsburgh, PA 15261, USA*
[b]*Division of General Internal Medicine, University of Pittsburgh School of Medicine, Pittsburgh, PA 15261, USA*
[c]*Department of Plastic Surgery, University of Pittsburgh and the McGowan Institute for Regenerative Medicine, Pittsburgh, PA 15261, USA*
[d]*University of Pittsburgh, Division of Endocrinology, Department of Medicine, Pittsburgh, PA 15261, USA*

Received 19 October 2021; received in revised form 24 November 2021; accepted 25 November 2021

KEY WORDS

Liver injury;
Leukemia;
Asparaginase;
Lipolysis;
Adverse drug reaction;
Adipose tissue;
Hepatic steatosis;
Amino acid response

Abstract PEGylated-L-asparaginase (PEG-ASNase) is a chemotherapeutic agent used to treat pediatric acute lymphoblastic leukemia (ALL). Its use is avoided in adults due to its high risk of liver injury including hepatic steatosis, with obesity and older age considered risk factors of the injury. Our study aims to elucidate the mechanism of PEG-ASNase-induced liver injury. Mice received 1500 U/kg of PEG-ASNase and were sacrificed 1, 3, 5, and 7 days after drug administration. Liver triglycerides were quantified, and plasma bilirubin, ALT, AST, and non-esterified fatty acids (NEFA) were measured. The mRNA and protein levels of genes involved in hepatic fatty acid synthesis, β-oxidation, very low-density lipoprotein (VLDL) secretion, and white adipose tissue (WAT) lipolysis were determined. Mice developed hepatic steatosis after PEG-ASNase, which associated with increases in bilirubin, ALT, and AST. The hepatic genes *Ppara*, *Lcad/Mcad*, *Hadhb*, *Apob100*, and *Mttp* were upregulated, and *Srebp-1c* and *Fas* were downregulated after PEG-ASNase. Increased plasma NEFA, WAT loss, and adipose tissue lipolysis were also observed after PEG-ASNase. Furthermore, we found that PEG-ASNase-induced liver injury was exacerbated in obese and aged mice, consistent with clinical studies of ASNase-induced liver injury. Our data suggest that PEG-ASNase-induced liver injury is due to drug-induced lipolysis and lipid redistribution to the liver.

*Corresponding author. Tel.: +1 412 383 8108.
E-mail address: chf63@pitt.edu (Christian A. Fernandez).
†These authors made equal contributions to this work.
Peer review under responsibility of Chinese Pharmaceutical Association and Institute of Materia Medica, Chinese Academy of Medical Sciences.

https://doi.org/10.1016/j.apsb.2021.11.022

1. Introduction

L-Asparaginase (ASNase) is one of the main antineoplastic agents used for the treatment of pediatric acute lymphoblastic leukemia (ALL). It is a non-human enzyme derived from bacterial (*Escherichia coli* or *Erwinia chrysanthemi*) sources that systemically depletes plasma and cerebral spinal fluid L-asparagine and leads to a decrease in protein synthesis and apoptosis among leukemia cells that have low asparagine synthetase (ASNS) expression[1]. ASNase derived from *E. coli* was approved by the U.S. Food and Drug Administration in 1978[2]; however, ASNase has been avoided in adult leukemia treatment regimens due to observations of acute liver injury in early adult trials during the late 1960s[3]. Adult ALL has relatively low survival rates compared to childhood ALL (*i.e.*, 40% *versus* over 90% survival, respectively[4]), and while adult and childhood ALL differ in the frequency of leukemias with poor genetic prognostic features, it is likely that the safe use of ASNase in adults would improve survival. Consistent with this hypothesis, among young adults and adolescent leukemia patients, several trials have been performed using pediatric or adult treatment regimens, including in the US, France, Holland, UK, and Italy[5−9], and all have demonstrated that protocols that include ASNase therapy yield superior 5-year survival.

ASNase-induced liver injury presents as abnormalities in plasma hepatic transaminases, such as aspartate aminotransferase (ALT), alanine aminotransferase (AST), alkaline phosphatase (ALP), and bilirubin[3]. The prevalence of transaminitis among children or adults receiving ASNase ranges from 35% to 45% for AST, 30%−35% for ALP, and 30%−60% for bilirubin[10−14]. Clinical studies have also indicated a higher incidence of ASNase-induced liver injury among patients receiving PEGylated versus non-PEGylated ASNase[15], suggesting that prolonged ASNase drug exposure may contribute to the risk of developing liver injury during therapy. Nevertheless, while drug exposure may play a role, liver injury is most common after one or two doses of PEG-ASNase[15], and similar associations were recently reported by the CALGB 9511 clinical study, which found that grade 4 hyperbilirubinemia occurred in 54% of patients who received 1−4 doses of PEG-ASNase[16]. The onset of liver injury correlates with the development of hepatic steatosis, including in a study of 31 pediatric patients which detected the presence of hepatic steatosis among 87% of patients receiving ASNase, indicating that the agent may induce fatty liver rather than liver injury being a pre-existing condition[17]. Concordant with clinical studies demonstrating that ASNase induces fatty liver, several preclinical investigations have also indicated that mice develop fatty liver after ASNase[18−23].

The mechanism by which asparagine depletion by ASNase leads to hepatic steatosis and liver injury is unclear. It has routinely been speculated to involve defects in liver mitochondrial β-oxidation, which would lead to the development of hepatic steatosis and consequently liver injury[24]. Limited research has investigated the mechanism of the toxicity, and no study has investigated whether ASNase impairs β-oxidation. The current study interrogates the mechanism of PEG-ASNase-induced liver injury in mice and supports the hypothesis that fatty acids mobilized from adipose tissue triglyceride stores lead to drug-induced liver injury. In contrast to current prevailing beliefs, we demonstrate that PEG-ASNase had no determinantal effect on the expression of genes involved in hepatic β-oxidation, VLDL secretion, and genes/proteins involved in lipid synthesis that would suggest liver injury.

2. Material and methods

2.1. Mice

Eight-week-old-male and female BALB/c and 8- and 72-week-old C57BL/6 male mice were purchased from Jackson Laboratories for our studies. All mice were housed in a specific pathogen-free animal facility under the care of the Division of Laboratory Animal Resources at the University of Pittsburgh with 12 h light and dark cycles. Upon arrival, mice were acclimated for a minimum of 3 days prior to all experiments. Mice were fed with *ad libitum* standard mouse chow diet and water except as detailed for obesity and pair-fed experiments. Pair-fed control mice received the same amount of food as that consumed by mice treated with PEG-ASNase. All animal experimental protocols were reviewed and approved by the University of Pittsburgh Institutional Animal Care and Use Committee and in compliance with the National Institutes of Health guide for the care and use of laboratory animals.

2.2. PEG-ASNase administration

Mice received a single dose of 1500 U/kg PEG-ASNase (Oncaspar®) or PBS vehicle control intraperitoneally and were euthanized at 1, 3, 5, or 7 days after administration. Blood, liver, and white adipose tissue (WAT) were collected after 6 h of fasting.

2.3. Induction of obesity

Obesity was induced by feeding 8-week-old C57BL/6 mice with a high fat diet (Envigo TD06414) that contains 60% kcal/g from fat. The mice were fed a high fat diet for 15 weeks, and obesity was confirmed by a glucose tolerance test, as described previously[25]. The mice were assigned into two treatment groups based on their glucose tolerance test results.

2.4. Measurement of hepatic biomarkers and non-esterified fatty acid (NEFA) concentrations in plasma

The plasma hepatic biomarkers AST, ALT, total and direct bilirubin, and plasma NEFA concentrations were measured using the

Randox Imola clinical chemistry analyzer (Randox, UK) as per the manufacturer's instructions.

2.5. Quantification of tissue triglyceride concentrations

Hepatic and muscle triglyceride concentrations were measured as described previously[26]. Briefly, the hepatic or muscle tissue was weighed and homogenized in a polystyrene tube containing 1 mL of 5% Nonidet-P40 (US Biological life sciences, N3500). The tissue homogenate was heated to 95 °C for 5 min and cooled for two cycles, and thereafter centrifuged for 5 min at 13,000 rpm. The supernatant was collected, and the concentration of triglycerides was measured using the Stanbio triglyceride assay kit (Stanbio laboratory, 2100-225). Tissue triglyceride levels are represented as mg/dL normalized by sample tissue weight.

2.6. Quantitative PCR analysis

Total RNA was extracted from frozen tissue using Trizol® reagent according to the manufacturer's protocol. The extracted RNA was tested for quality by measuring A260/280 ratio, and 1 μg of RNA was used to synthesize cDNA using the High-Capacity cDNA Reverse Transcription Kit (Applied Biosystems). Gene expression was quantified in the liver and WAT using SYBR® green on a QuantStudio 6 Flex Real-Time PCR system. Primer sequences used in this study are provided in Supporting Information Table S1. Gene expression was normalized to that of the housekeeping gene cyclophilin A. Relative gene expression is reported as fold-change compared to control at the same timepoint.

2.7. Western blot analysis

The immunoblot analysis of liver and WAT was performed as previously described[27]. Briefly, protein lysates from homogenized tissues were prepared using RIPA buffer with protease and phosphatase inhibitor. Protein concentrations were measured by Pierce BCA assay and normalized. Samples were loaded on Mini-Protean TGX 4%−15% pre-cast gels (BIO-RAD). After electrophoresis, wet transfer was performed onto 0.22 μm PVDF membranes and blocked with 5% non-fat milk or 5% bovine serum albumin for phosphorylated proteins. After blocking, the membrane was probed with primary antibodies overnight followed by incubation for 1 h at room temperature with anti-rabbit or anti-mouse horseradish peroxidase conjugated secondary antibodies with intermittent washing steps in between with tris-buffered saline containing Tween 20. Protein bands were visualized with Super Signal West Pico Plus chemiluminescent substrate (Thermo Fisher Scientific).

2.8. Cell culture and 3T3-L1 adipocyte differentiation protocol

HepG2 human hepatocellular carcinoma cells and undifferentiated 3T3-L1 mouse embryonic fibroblast cells were grown in a DMEM medium supplemented with 10% fetal bovine serum, penicillin (100 U/mL) and streptomycin (100 μg/mL) at 37 °C in humidified air with 5% CO_2. To differentiate 3T3-L1 cells into adipocytes, cells were harvested and plated in 6 well plates for differentiation. Once cells reached 70% confluency, they were treated with 0.5 mmol/L isobutylmethylxanthine, 1 μmol/L dexamethasone, and 10 μg/mL insulin[28]. After 3 days, the induction media was replaced with an insulin medium containing 10 μg/mL of insulin for 3 additional days. Cells were then maintained in maintenance media, consisting of DMEM medium supplemented with 10% calf bovine serum, penicillin (100 U/mL) and streptomycin (100 μg/mL). Differentiated adipocytes were treated with 0.1 U/mL of PEG-ASNase or 50 μg/mL cycloheximide for 24 h[29]. After 24 h of treatment, the conditioned media and cellular protein were harvested and assayed for NEFA concentration and protein expression, respectively.

2.9. Statistical analysis

All results are expressed as mean ± standard deviation. Statistical significance was determined using Student *t*-tests. GraphPad Prism 8.4 (GraphPad Software, CA, USA) was used to perform the analyses.

3. Results

3.1. Mice developed hepatic steatosis, hyperbilirubinemia, and elevated liver enzymes in plasma 3 days after receiving a single dose of PEG-ASNase

Mice receiving PEG-ASNase developed pale-colored livers, and consistent with their appearance, hepatic triglycerides were elevated ~5-, 4-, and 3-fold at 3, 5, and 7 days after PEG-ASNase administration, respectively (Fig. 1A and B, $P < 0.001$). However, there was no evidence of fatty liver at day 1 post-PEG-ASNase administration. The extent and severity of fatty liver, as determined by H&E and Oil Red O staining, were similar 3−7 days after PEG-ASNase (Fig. 1A). Furthermore, mice experienced on average 10% loss in body weight and >20% loss in liver weight 3−5 days after receiving PEG-ASNase (Supporting Information Fig. S1A and S1B, $P < 0.0001$). Blood chemistry analysis of plasma samples indicated that mice developed statistically elevated total bilirubin 1 day after PEG-ASNase (Fig. 1C) and more severe hyperbilirubinemia (>10-fold, $P < 0.001$) 3−7 days after the drug administration (Fig. 1C and D). Interestingly, PEG-ASNase administration showed a stronger effect on direct (conjugated) bilirubin levels rather than indirect (unconjugated) bilirubin, suggesting that PEG-ASNase may impair bilirubin transport rather than its conjugation. In addition, we found a ~2-fold increase ($P < 0.001$, Fig. 1E and F) in ALT and AST concentrations 3, 5, or 7 days after PEG-ASNase, consistent with the onset of fatty liver. Furthermore, analyses of plasma drug levels 1−7 days after PEG-ASNase administration indicated that mice had drug exposures within clinical therapeutic ranges (Fig. S1C)[30]. Our results demonstrate that our murine model of PEG-ASNase-induced liver injury is similar to the clinical adverse drug reaction observed in adult leukemia patients receiving this chemotherapeutic agent[31].

3.2. PEG-ASNase treatment increased the expression of markers of β-oxidation and decreased the expression of markers of fatty acid synthesis in the liver

Several case studies have suggested that ASNase-induced hepatotoxicity is due to a decrease in mitochondrial β-oxidation of fatty acids[24]. To thoroughly investigate the possible mechanisms leading to the development of PEG-ASNase-induced liver injury using our murine model, the expression of genes involved in lipid synthesis, very-low-density lipoprotein (VLDL) secretion, and β-oxidation was measured 1−7 days after PEG-ASNase administration (Fig. 2A−C). Our data indicate that at all time points, genes involved in lipid synthesis, including *Srebp-1c*,

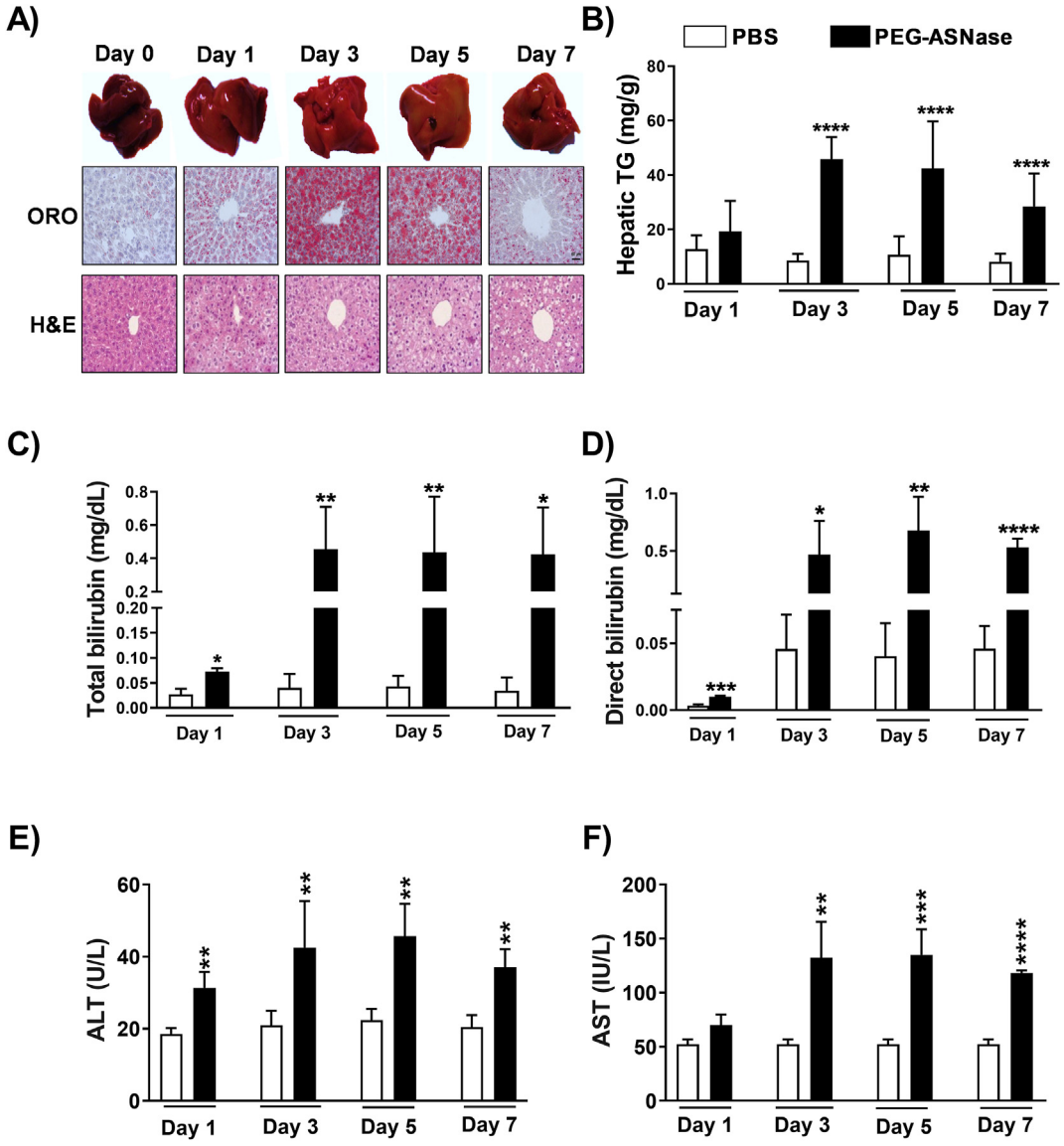

Figure 1 PEG-ASNase in mice leads to fatty liver and liver injury. (A) Oil red O (ORO) and H&E staining of liver samples collected from mice receiving 1500 U/kg of PEG-ASNase (Days 1, 3, 5 and 7) indicate the development of hepatic steatosis relative to controls. (B) Mice receiving PEG-ASNase had ~5-, 4-, and 3-fold higher triglyceride (TG) concentrations at 3, 5, and 7 days after treatment, respectively. (C−F) Plasma total/direct bilirubin, alanine transaminase (ALT), and aspartate transaminase (AST) levels were higher in PEG-ASNase-treated mice compared to controls. Data is the mean ± SD with statistical significance indicated as **** for $P < 0.0001$, *** for $P < 0.001$, ** for $P < 0.01$, and * for $P < 0.05$. Data from $n \geq 30$ mice. Scale bar in (A) indicates 50 μm.

Fas, and *Scd-1* were downregulated ($P < 0.001$, Fig. 2A), the expression of genes involved in β-oxidation, including *Ppara*, *Lcad*, and *Mcad*, were upregulated ($P < 0.001$, Fig. 2B), and genes involved in hepatic VLDL secretion or lipid transport, such as *Apob100* and *Mttp*, were upregulated ($P < 0.001$, Fig. 2C) after PEG-ASNase treatment in mice. We confirmed our gene expression results by measuring the protein levels of SREBP-1c, FAS, PPARα, HADHB (a PPARα target gene that catalyzes the final step of β-oxidation[32]), APOB100 and MTTP (Fig. 2D). Consistent with the gene expression analysis, we found that the levels of proteins involved in lipid synthesis were downregulated, whereas the levels of proteins involved in β-oxidation and VLDL secretion were upregulated after PEG-ASNase (Fig. 2D). Furthermore, we found a similar effect of PEG-ASNase on HepG2 cells and primary murine hepatocytes treated with PEG-ASNase at clinically relevant concentrations (Fig. 2E and F)[33], except for PPARα, which was downregulated by PEG-ASNase in HepG2 cells and primary murine hepatocytes and contrary to our *in vivo* observations. Supporting our hypothesis that the pharmacological action of PEG-ASNase on the liver does not directly lead to hepatic steatosis, the triglyceride levels in HepG2 cells and primary murine hepatocytes were not affected after treatment with PEG-ASNase (Supporting Information Fig. S2A and S2B), despite the decrease in proteins involved in β-oxidation. Taken together, our data suggest that the hepatic steatosis developed in mice receiving PEG-ASNase is not due to altered hepatic lipid synthesis, β-oxidation, VLDL secretion, or the direct effect of PEG-ASNase on hepatocytes. Rather, we hypothesized that the hepatic steatosis and increased expression of genes involved in β-oxidation are likely

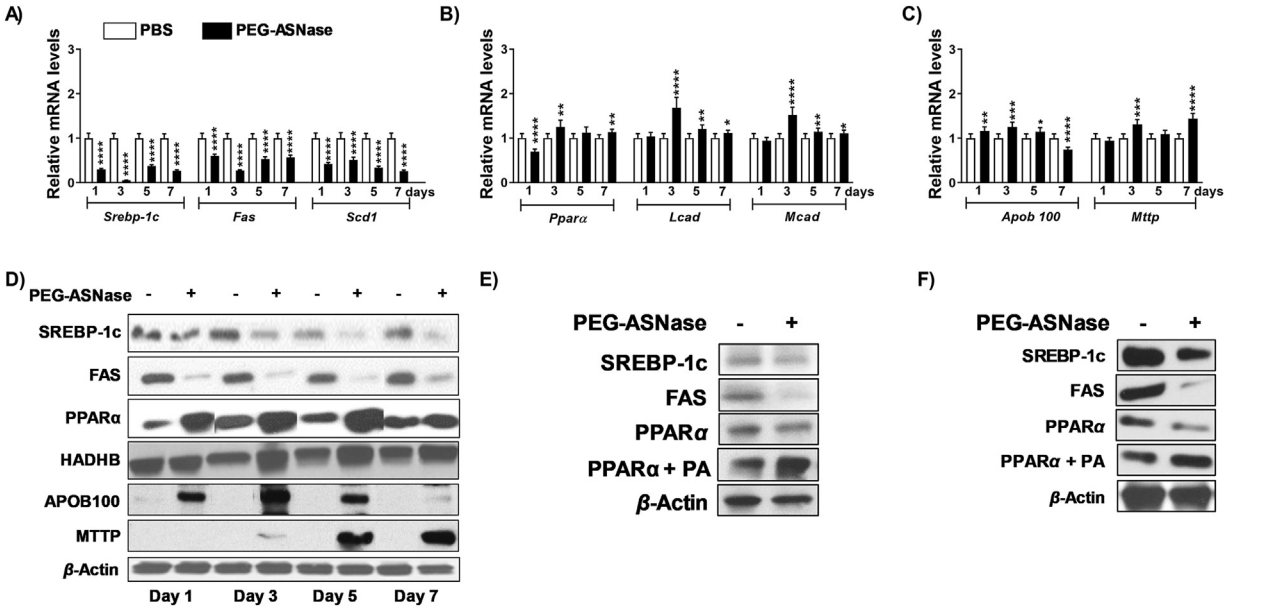

Figure 2 The effect of PEG-ASNase on the liver of mice does not explain the drug-induced liver injury. Hepatic RNA from mice treated with PEG-ASNase or PBS control was used to assess its effect on genes involved in lipid synthesis, β-oxidation, or very-low density lipoprotein (VLDL) secretion. (A) PEG-ASNase led to a decrease in the expression of genes involved in lipid synthesis (*Srebp-1c*, *Fas*, and *Scd1*), (B) an increase in the expression of genes involved β-oxidation (*Ppara*, *Lcad*, and *Mcad*), and (C) a decrease in the expression of genes involved VLDL secretion (*Apob100*, and *Mttp*). (D) The hepatic protein levels of SREBP-1c and FAS proteins levels were downregulated, whereas PPARα, HADHB, APOB100, and MTTP were increased relative to controls. (E) In HepG2 cells and (F) murine primary hepatocytes, PEG-ASNase (0.1 U/mL) decreased the protein levels of SREBP-1c, FAS, and PPARα, whereas 3 mmol/L palmitic acid (PA) along with PEG-ASNase increased PPARα protein levels. Data is the mean $\pm$ SD with statistical significance indicated as **** for $P < 0.0001$, *** for $P < 0.001$, ** for $P < 0.01$, and * for $P < 0.05$. Data in (A)−(C) from $n \geq 30$ mice.

indirect and due to the observed effect of PEG-ASNase on non-hepatic tissues.

3.3. *PEG-ASNase leads to induction of lipolysis in adipose tissue and adipocytes*

Interestingly, we found that mice receiving PEG-ASNase experienced a >40% reduction of WAT ($P < 0.001$, Fig. 3A), which was associated with increased plasma NEFA concentrations ($P < 0.001$, Fig. 3B) and increased muscle triglycerides ($P < 0.01$, Fig. 3C). Therefore, we hypothesized that PEG-ASNase induced WAT lipolysis, which led to a redistribution of fatty acids and the development of hepatic steatosis. Because *Atgl* and *Hsl* encode lipases essential for lipolysis and fatty acid mobilization, we measured their gene expression in WAT and found that they were both upregulated after PEG-ASNase (Fig. 3D). Similarly, ATGL, HSL, and phosphorylated HSL protein levels were increased relative to controls (Fig. 3E, Day 3). In agreement with our *in vivo* study, we also found that PEG-ASNase upregulated ATGL and phosphorylated-HSL protein levels *in vitro* using differentiated 3T3-L1 adipocytes (Fig. 3F) and resulted in increased media free fatty acid concentrations compared to controls (Fig. 4A). Taken together, our data suggest that PEG-ASNase induces adipose tissue lipolysis, and increases fatty acid uptake by the liver, resulting in the development of hepatic steatosis. Because fatty acids can upregulate *Ppar*α[34] and because we observed conflicting results regarding the effect of PEG-ASNase on PPARα *in vivo versus in vitro* (Fig. 2E and F), we next treated HepG2 cells and murine primary hepatocytes with 3 mmol/L palmitic acid and 0.1 U/mL PEG-ASNase to better recapitulate *in vivo* conditions with circulating NEFA. We found that PEG-ASNase along with palmitic acid increases PPARα protein levels relative to controls (Fig. 2E and F). Therefore, the increased PPARα signaling detected *in vivo* (Fig. 2D) is likely due to drug-induced lipolysis rather than to the direct effect of PEG-ASNase on hepatic PPARα and β-oxidation.

PEG-ASNase treatment in mice led to decreased food intake compared to non-treated control mice (Supporting Information Fig. S3A). To determine whether the decrease in food intake could drive the effects of PEG-ASNase on the liver and adipose tissue, we performed pair-fed studies. While pair-feeding led to a loss in body weight that was less severe than PEG-ASNase treatment (Fig. S3B), the decreased food intake did not have a corresponding effect on hepatic triglyceride concentrations (Fig. S3C), plasma bilirubin (Fig. S3D and S3E), or ALT (Fig. S3F) compared to control mice. Furthermore, we detected no difference in hepatic SREBP-1c or FAS protein levels in pair-fed mice relative to controls (Fig. S3G and S3H). Consistent with these results, we did not detect any significant WAT loss, changes in plasma NEFA, increases in muscle triglyceride levels, or differences in ATGL, HSL, or p-HSL protein levels (Fig. S4A−S4F). These results suggest that the decreased food intake is not responsible for the effect of PEG-ASNase on the liver or adipose tissue.

3.4. *PEG-ASNase-induced adipose tissue lipolysis and release of NEFA is associated with activation of eIF2α and protein kinase A (PKA) in adipocytes*

No previous study has indicated that PEG-ASNase treatment leads to adipocyte lipolysis. We, nevertheless, hypothesized that the

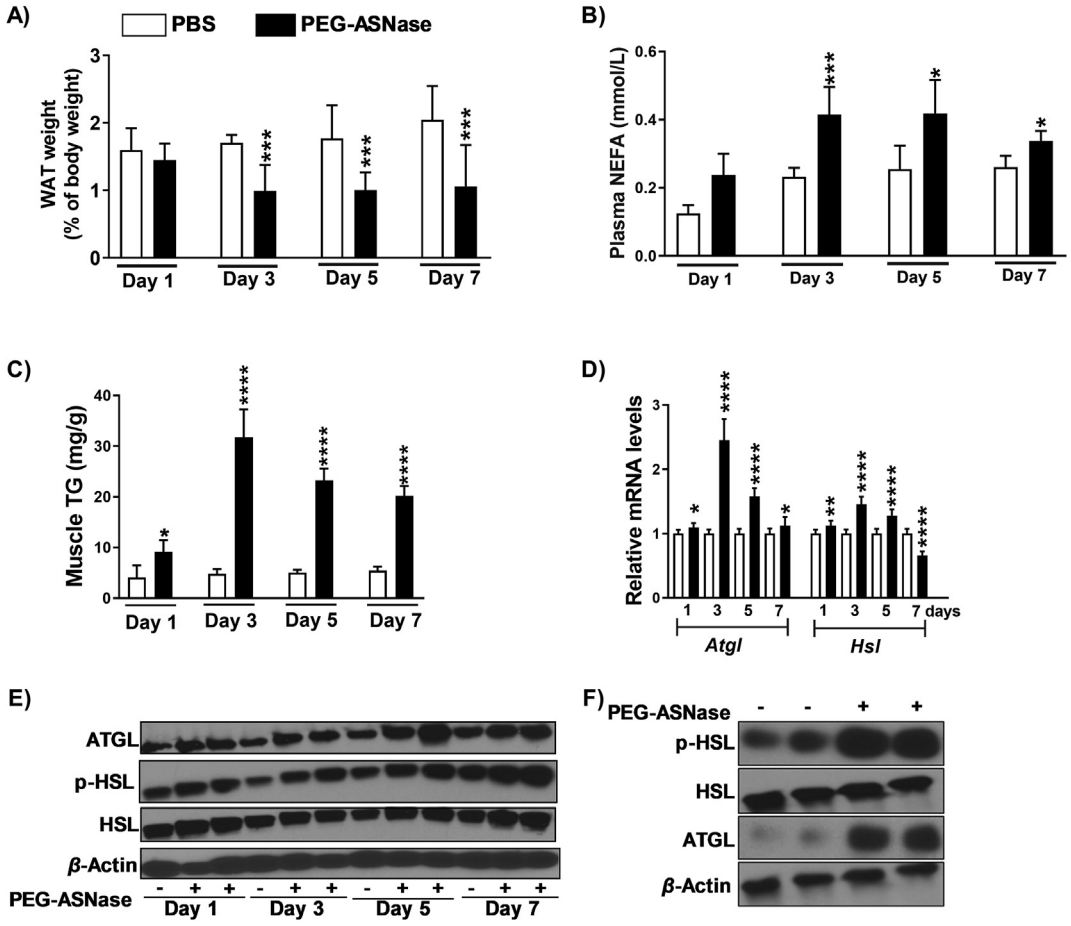

Figure 3 PEG-ASNase liver injury is associated with adipose tissue lipolysis. (A) Mice receiving PEG-ASNase experienced a significant loss in white adipose tissue (WAT), (B) had elevated plasma non-esterified fatty acid (NEFA) concentrations, and (C) had increased muscle triglyceride (TG) levels relative to controls, consistent with the induction of WAT lipolysis. (D) The mRNA levels of *Atgl* and *Hsl* in WAT were increased in treated mice compared to controls, with (E) corresponding observations in the protein levels of phosphorylated HSL (p-HSL), HSL, and ATGL (Day 3). (F) PEG-ASNase (0.1 U/mL) had a similar effect on p-HSL, HSL, and ATGL in 3T3-L1 differentiated adipocytes. Data is the mean ± SD with statistical significance indicated as **** for $P < 0.0001$, *** for $P < 0.001$, ** for $P < 0.01$, and * for $P < 0.05$. Data in (A)−(D) from $n \geq 30$ mice.

mechanism of PEG-ASNase-induced adipocyte lipolysis is due to asparagine depletion and the induction of the amino acid response pathway, which is dependent on the phosphorylation of the α subunit of the eukaryotic translation initiation factor 2 (eIF2α) by the general control nonderepressible 2 (GCN2) kinase[35]. To identify whether this mechanism is involved in PEG-ASNase-induced adipocyte lipolysis, we measured p-eIF2α *in vivo* and *in vitro* in WAT after PEG-ASNase exposure and in differentiated 3T3-L1 adipocytes, respectively. We found that PEG-ASNase treatment is associated with increased phosphorylation of eIF2α in WAT and in 3T3-L1 adipocytes (Fig. 4B and C). Because eIF2α can also be phosphorylated *via* other mechanisms[36], we also treated 3T3-L1 differentiated adipocytes with cycloheximide, which is known to induce high levels of eIF2α phosphorylation by protein kinase R (PKR)-like endoplasmic reticulum kinase (PERK)[37]. Like PEG-ASNase treatment, we found that cycloheximide led to elevated p-eIF2α, induction of ATGL and p-HSL, and higher media NEFA concentrations relative to control cells *in vitro* (Fig. 4A and D). Our results suggest that the mechanism of adipocyte lipolysis induced by PEG-ASNase is dependent on the phosphorylation of eIF2α.

To understand the relation between phosphorylation of eIF2α and the activation of the lipolytic proteins ATGL and HSL, we investigated the expression of PKA in adipocytes and WAT. Interestingly, the p-PKA protein levels were increased in WAT and 3T3-L1 adipocytes after PEG-ASNase (Fig. 4B and C). Our observation suggests that the PEG-ASNase-induced adipose tissue lipolysis is associated with the activation of the eIF2α−PKA−ATGL−HSL axis in adipose tissue *via* a currently unknown mechanism.

3.5. *PEG-ASNase-induced hepatic steatosis is exacerbated in obese and aged mice*

Two known clinical risk factors of PEG-ASNase-induced hepatotoxicity are obesity and older age[3,38,39]. Based on our results and clinical findings, we hypothesized that obesity exacerbates PEG-ASNase liver injury due to increased adiposity, whereas older age aggravates the toxicity due to the effect of aging on hepatic PPARα protein levels and thereby β-oxidation. To test our hypothesis, we investigated the effect of obesity or older age on PEG-ASNase-induced liver injury using obese[20] or 72-week-old[40]

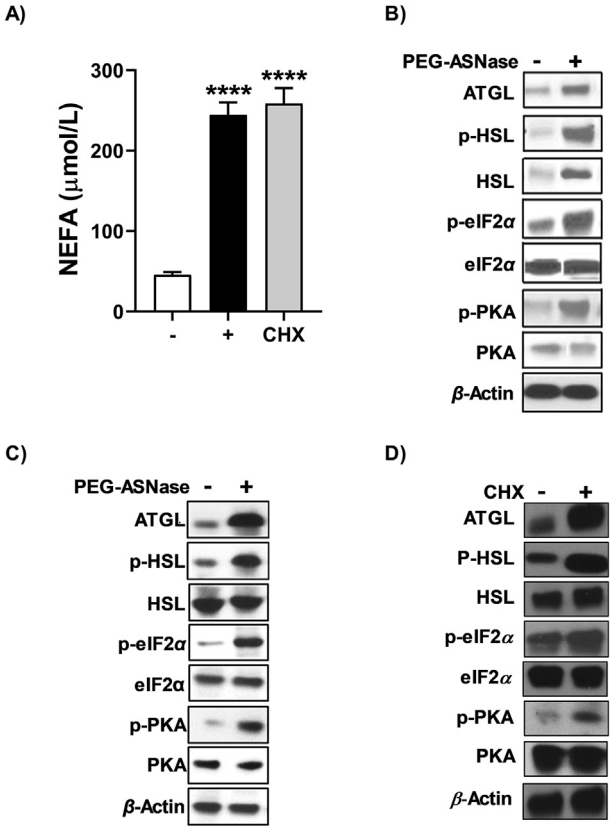

Figure 4 PEG-ASNase- and cycloheximide-induced lipolysis is associated with phosphorylation of eIF2α. (A) The NEFA concentrations in the conditioned media of differentiated 3T3-L1 cells were elevated after PEG-ASNase (0.1 U/mL) and cycloheximide (CHX, 50 μg/mL) treatment. The protein levels of p-eIF2α, p-PKA, ATGL, and p-HSL in (B) WAT and (C) differentiated 3T3-L1 adipocytes were upregulated after PEG-ASNase. (D) Treating differentiated 3T3-L1 cells with cycloheximide leads to a similar increase in ATGL, p-HSL, p-eIF2α, and p-PKA as PEG-ASNase. Data is the mean ± SD with statistical significance indicated as **** for $P < 0.0001$. Data in (A) representative of 3 independent experiments.

C57BL/6 male mice, where 72-week-old mice, but not younger aged mice, develop impaired β-oxidation[41,42,43].

Obesity was induced in male mice using a high fat diet for 15 weeks, where the onset of obesity was confirmed *via* the development of insulin resistance measured by an oral glucose tolerance test and area under curve (AUC) values (Supporting Information Fig. S5A and S5B). Obese mice thereafter received PEG-ASNase and were sacrificed 3 days after drug administration. PEG-ASNase treatment led to nearly a 20% loss of body weight (Fig. 5A) and to a significant loss in WAT relative to obese control mice (Fig. S5C). We found that the livers of obese mice receiving PEG-ASNase appeared more pale than non-obese control mice that were also treated with PEG-ASNase. Consistently, the hepatic triglyceride concentrations of obese mice receiving PEG-ASNase were ~4-fold higher than control obese (Fig. 5B, $P < 0.001$) and PEG-ASNase treated non-obese mice (Fig. 1B). Furthermore, the direct bilirubin concentrations were >25-fold higher in obese PEG-ASNase treated mice compared to obese controls (Fig. 5C, $P < 0.01$) and >2-fold higher than PEG-ASNase treated non-obese mice.

Using 72-week-old C57BL/6 male mice, we first confirmed that aging decreases PPARα and HADHB protein levels relative to 8-week-old control mice (Fig. 5D)[44]. We thereafter treated aged mice with PEG-ASNase, and at Day 3 post-drug administration, we found that mice lost similar body weight as non-aged mice (Fig. 5A), whereas the hepatic triglyceride levels were elevated 2.5-fold compared to age-matched controls (Fig. 5B, $P < 0.01$) and 2-fold relative to 8-week-old mice receiving PEG-ASNase (Fig. 1B). Furthermore, the plasma direct bilirubin concentrations were elevated 6.5-fold compared to age-matched controls (Fig. 5C, $P < 0.01$) and 2.5-fold relative to 8-week-old mice receiving PEG-ASNase (Fig. 1D). PEG-ASNase treatment induced PPARα levels in aged mice relative to PBS controls, albeit the PPARα induction was significantly attenuated compared to non-aged mice (Fig. 5D). Hence, our murine model of PEG-ASNase-induced liver injury recapitulates the clinical liver injury seen in leukemia patients, including potentiation by risk factors. Altogether, our results support that PEG-ASNase liver injury is due to adipocyte lipolysis and that factors affecting the disposition or quantity of fatty acids liberated upon lipolysis have a corresponding effect on the severity of liver injury.

4. Discussion

PEG-ASNase is one of the main drugs used to treat pediatric ALL, and although it is also effective against adult ALL, dose-limiting liver injury restricts its use. However, the mechanism of this adverse drug reaction is not well-understood. Our study aimed to recapitulate and elucidate the mechanism of this adverse drug

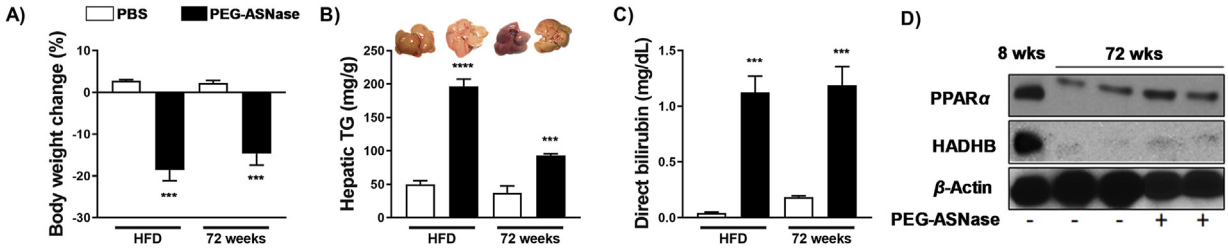

Figure 5 PEG-ASNase-induced liver injury is exacerbated in obese and 72-week-old mice. Obese and aged (72-week-old) mice receiving PEG-ASNase (A) lost over 10% of their body weight, (B) had elevated hepatic triglyceride (TG) concentrations (representative pictures of livers from different treatment groups are shown in the upper panel), and (C) higher plasma direct bilirubin concentrations compared to obese or age-matched control mice, respectively. (D) Aged mice had lower PPARα and HADHB protein levels compared to 8-week-old mice, which were slightly elevated after PEG-ASNase treatment. Data in (A)−(C) from $n \geq 3$ mice per group.

reaction in a murine model, where mice treated with clinically relevant doses of PEG-ASNase achieved therapeutic plasma drug levels (Fig. S1C)[33] and developed fatty livers (Fig. 1A and B) that were associated with a 2−8-fold increase in liver function test values (Fig. 1C−F), similar to clinical ASNase liver injury[10−14]. Surprisingly, we found no evidence that PEG-ASNase-induced liver injury was due to the direct effect of the chemotherapeutic agent on the liver or hepatocytes (Fig. 2F and Fig. S2A). Rather, we found evidence that PEG-ASNase liver injury is due to its effect on adipose tissue, with mice losing >40% of WAT (Fig. 3A) and having elevated plasma NEFA concentrations 3 days after the drug administration (Fig. 3B). Consistent with our hypothesis, we also demonstrate that PEG-ASNase treatment in mice is associated with markers of adipose tissue lipolysis (Fig. 3D−F) and that the chemotherapeutic agent directly leads to the activation of lipolysis in 3T3-L1 adipocytes (Fig. 4A). Based on the results of our study, we posit that the PEG-ASNase-induced liver injury observed in mice is due to NEFA mobilization from adipose tissue and that factors that alter hepatic NEFA disposition can exacerbate the severity of the adverse drug reaction. Our study is the first to investigate the mechanism of PEG-ASNase-induced liver injury and to assess the effect of the drug on adipose tissue.

Although few studies have investigated the mechanism of PEG-ASNase-induced liver injury, several clinical case studies have suggested that the injury is due to drug-induced inhibition of protein synthesis leading to defective hepatic β-oxidation and toxicity *via* decreased protein levels of PPARα[24]. We directly investigated this hypothesis and found that PPARα is elevated in PEG-ASNase treated mice relative to controls (Fig. 2B and D), albeit PPARα protein levels were decreased in primary murine hepatocytes after PEG-ASNase treatment (Fig. 2F). Nevertheless, we show that the direct effect of PEG-ASNase on PPARα is dependent on fatty acid concentrations, where treating primary murine hepatocytes with palmitic acid and PEG-ASNase leads to an upregulation of PPARα, suggesting that the increased hepatic PPARα levels in mice were due to fatty acid mobilization. We also demonstrate that PEG-ASNase does not alter the expression of genes involved in fatty acid synthesis or VLDL secretion in a manner that would explain the observed hepatic steatosis and liver injury (Fig. 2A and C). Rather, we show that PEG-ASNase treated primary murine hepatocytes do not develop increased hepatocyte triglyceride concentrations relative to vehicle control cells (Fig. S2A). Interestingly, while we observe an increase in hepatic triglyceride levels in our murine model, we concurrently see a loss in liver weight (Fig. S1B). Clinical asparaginase toxicology studies support that the weight loss may be due to depletion of hepatic glycogen stores[45]. However, the detailed mechanism of PEG-ASNase-induced liver weight loss in our mouse model remains to be defined. Collectively, the results from our study contrast with clinical case studies suggesting that the mechanism of ASNase-induced liver injury is due to the effect of the agent on the liver and fatty acid oxidation.

The release of NEFA from triglycerides during lipolysis is a multistep process. Adipose triglyceride lipase (ATGL) performs the first step of triglyceride hydrolysis[46]. Phosphorylated HSL proceeds to hydrolyze diglycerides to monoglycerides, which are hydrolyzed by monoglyceride lipase (MGL) to fatty acids and glycerol. Given the rapid and substantial decrease in WAT after PEG-ASNase treatment (Fig. 3A), we assessed adipose tissue lipolysis signaling and found that mice receiving PEG-ASNase had higher p-HSL and ATGL relative to controls (Fig. 3E). Supporting that PEG-ASNase directly leads to lipolysis, 3T3-L1 adipocytes treated with PEG-ASNase had higher protein levels of p-PKA, p-HSL, and ATGL (Fig. 4C), which is similar to our *in vivo* WAT samples (Fig. 4B) and led to higher NEFA concentrations in the cultured media of these cells relative to controls (Fig. 4A). Our results are consistent with previous studies investigating the effect of leucine, isoleucine, or valine deprivation on fat mass and lipid metabolism[47,48]. Our results are also consistent with a recent metabolomics study of pediatric plasma samples collected after the completion of the induction phase of leukemia therapy, which found that fatty acid concentrations were increased after induction and that lipid metabolism was the most significantly altered pathway in a pathway enrichment analysis[49]. Interestingly, we see a decrease in hepatic triglyceride levels and ORO staining (Fig. 1A and B), whereas our H&E analysis suggests the persistence of fatty liver (Fig. 1A, Day 7). While our clinical research supports mobilization of lipid-based moieties, particularly the membrane lipid phosphatidylethanolamine (PE) plasmalogen[49], additional studies are required to elucidate the hepatic lipids accumulating after PEG-ASNase treatment. Altogether, our results, and that of others, support that the fatty liver induced by PEG-ASNase is most likely due to hepatic fatty acid accumulation following drug-induced adipose tissue lipolysis. Nevertheless, the mechanism by which PEG-ASNase leads to ATGL activation and induction of lipolysis is not clear.

Based on our proposed mechanism of PEG-ASNase-induced liver injury, it is likely that multiple mechanisms can exacerbate the toxicity after drug exposure. Obesity and older age are two known clinical risk factors of ASNase-induced liver injury in adults[3,15,50] and children[39]. Therefore, it is important to determine whether PEG-ASNase can be safely incorporated during ALL

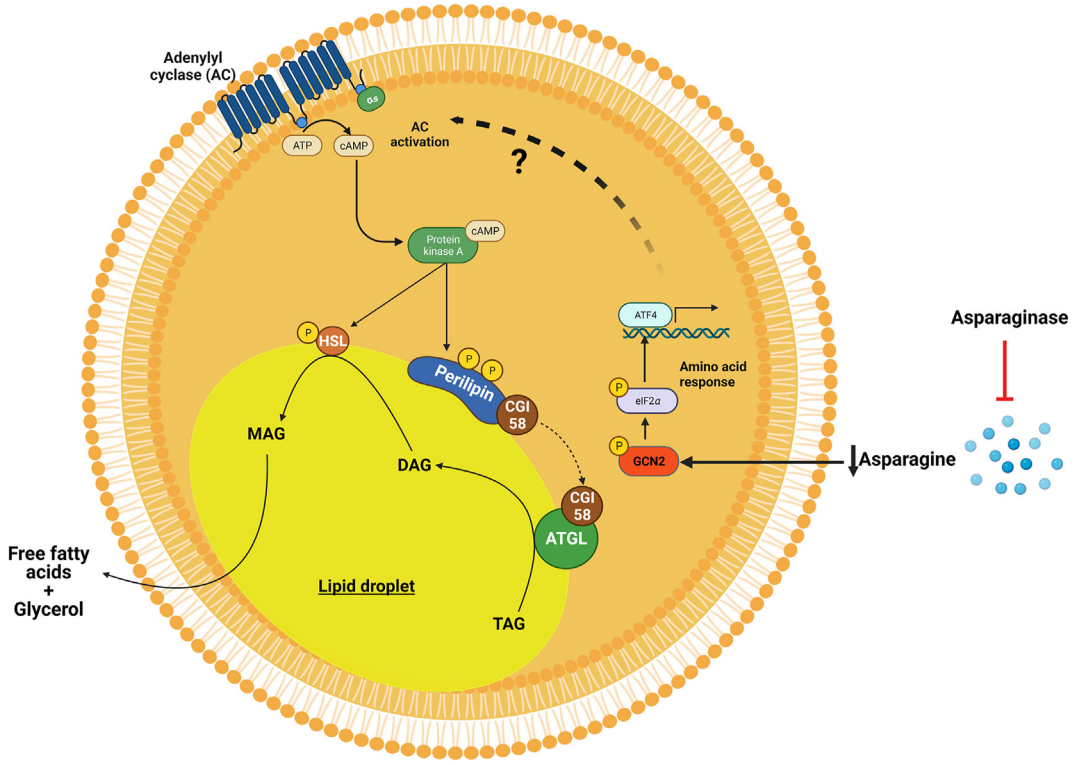

Figure 6 PEG-ASNase leads to adipose tissue lipolysis *via* an unknown mechanism. PEG-ASNase leads to asparagine depletion that induces general control nonderepressible 2 (GCN2) kinase-dependent activation of the amino acid response (AAR) *via* phosphorylation of eIF2α. We hypothesize that the AAR leads to activation of adenylyl cyclase due to our studies indicating that PEG-ASNase or cycloheximide treatment, which both induce phosphorylation of eIF2α, leads to activation of PKA and HSL. Altogether, we posit that PEG-ASNase-induced liver injury is due to ATGL activation by the chemotherapeutic agent. Figure created with BioRender.com.

treatment among patients with these risk factors. Two recent studies have attempted to detect age-related differences in ASNase liver injury using 35 or 16-week-old mice[22,51], but no study has been able to replicate the clinical association with age, likely due to a lack of clarity on the mechanism of PEG-ASNase-induced liver injury. Similar to the effects of aging on β-oxidation in humans, 18-month-old (72-week-old) aged mice have lower protein levels of PPARα and its target gene HADHB, which catalyzes the final step of β-oxidation, relative to 8-week-old control mice (Fig. 5D)[44]. Therefore, we hypothesized that older age is a risk factor of PEG-ASNase-induced liver injury due to decreased β-oxidation. Consistent with our hypothesis, we found that aged mice receiving PEG-ASNase were sensitized to liver injury, where aged mice developed 2-fold higher hepatic triglyceride levels relative to younger mice (*i.e.*, 8-week-old) receiving PEG-ASNase (Figs. 5B and 1B). Nevertheless, because aged mice were only available on a C57BL/6 background, it is possible that the magnitude of PEG-ASNase-induced liver injury may differ by mouse strain[52]. However, our preliminary data indicate that 8-week-old C57BL/6 are equally sensitive to PEG-ASNase-induced liver injury as their BALB/c counterparts (Supporting Information Fig. S6).

Plasma NEFA concentrations are commonly elevated in obese individuals due to a decrease in insulin-mediated suppression of lipolysis[53], where excessive NEFA will be re-esterified, metabolized, or can lead to lipotoxicity[54]. Therefore, we speculated that obese mice are sensitized to PEG-ASNase-induced liver injury due to higher basal fatty acid concentrations and more adipose tissue, which can lead to more hepatic fatty acid accumulation after PEG-ASNase relative to non-obese controls. Consistent with our hypothesis, obese mice receiving PEG-ASNase lost nearly 20% body weight relative to control obese mice (Fig. 5A), which was more severe relative to non-obese WT mice (Fig. S1A) and developed severe hepatic steatosis with >4-fold higher hepatic triglyceride levels relative to non-obese mice receiving PEG-ASNase (Figs. 5B and 1B). Overall, our murine model of PEG-ASNase-induced liver injury recapitulates clinical ASNase liver injury, including exacerbation by clinical risk factors. Based on our proposed mechanism of PEG-ASNase-induced liver injury (Fig. 6), we anticipate that the severity of injury correlates with adiposity and age. Similarly, we anticipate that any other factors affecting the disposition of hepatic FFAs have a corresponding effect on the severity of PEG-ASNase-induced liver injury. This suggests that increasing FFA oxidation (*e.g.*, using fenofibrate) can attenuate the severity of PEG-ASNase-induced liver injury, whereas patients with multiple risk factors (*e.g.*, obesity and older age) can have additive effects on the severity and risk of developing the adverse drug reaction.

The role of the eIF2α/GCN2 kinase axis on the response or adaptation of hepatocytes to amino acid depletion by ASNase has been previously investigated[19–21,35,55]. These studies have demonstrated that dysregulation of genes involved in fatty acid synthesis, oxidation, uptake, and secretion protects the liver from drug-induced DNA damage and cell death[19,21]. Consistent with GCN2 playing a protective role from PEG-ASNase-induced toxicity in hepatocytes, we found that PEG-ASNase treatment in primary

hepatocytes does not lead to triglyceride accumulation (Fig. S2A). Nevertheless, our research is the first to suggest that GCN2 in adipose tissue plays a pathologic role during ASNase therapy. That is, amino acid depletion in the adipose tissue leads to ATGL activation, induction of lipolysis, and hepatic fatty acid accumulation (Fig. 6). Our results (Figs. S3 and S4), which agree with that of others, demonstrate that the effect of PEG-ASNase on liver injury is not due to decreased food intake[19–21,35,55]. Additional studies are required to confirm that PEG-ASNase activates ATGL and to elucidate the mechanism by which amino acid depletion leads to ATGL activation. Furthermore, additional mechanistic studies are required to identify a pharmacological target that can prevent PEG-ASNase-induced adipose tissue lipolysis while retaining the protective role of GCN2 in hepatocytes.

Our studies suggest that targeting ATGL activity or its activation can mitigate PEG-ASNase-induced liver injury by modulating adipose tissue lipolysis (Fig. 6). In contrast, inhibiting GCN2 may prevent adipose tissue lipolysis, but induce hepatotoxicity[19]. Furthermore, the effects of pharmacological inhibition of a prospective target in leukemias is essential to verify that rescuing from the drug-induced liver injury does not compromise treatment efficacy. Rather, it would be ideal if a target that prevents PEG-ASNase-induced liver injury also possesses antileukemic efficacy. Because PEG-ASNase-induced lipolysis also drives the exacerbated liver injury in obese and aged mice, inhibiting ATGL or its activation would provide a safe strategy for using this agent in patients at high risk of this adverse drug reaction. Our studies also support that managing obesity may decrease the risk of developing PEG-ASNase-induced liver injury in ALL patients. Furthermore, future studies investigating the concomitant effect of PEG-ASNase and glucocorticoids, which can induce adipose tissue lipolysis and activate ATGL[56], will be critical for best mitigating the risk of PEG-ASNase liver injury in ALL patients.

5. Conclusions

In summary, our research is the first to investigate the mechanism of PEG-ASNase-induced liver injury and to suggest that the drug-induced liver injury is due to its effect on adipose tissue and lipolysis induction. Our methods used physiologically relevant doses and concentrations of PEG-ASNase to best investigate the mechanism of the drug-induced liver injury. We posit that fatty acids liberated during adipose tissue lipolysis accumulate in the liver, and those not re-esterified to triglyceride or metabolized for energy production lead to liver injury. While further mechanistic experiments are required to demonstrate GCN2-dependent ATGL activation, our results suggest that hepatic GCN2 protects from PEG-ASNase-induced liver injury, whereas GCN2 in the adipose tissue plays a pathological role in the drug-induced liver injury. These studies can extend the therapeutic benefit of ASNase by identifying pharmacological targets that can be used to inhibit ATGL activation during the amino acid response and protect ALL patients from PEG-ASNase-induced liver injury.

Acknowledgments

This work was supported by the National Institutes of Health grants CA216815 and TL1TR001858 (USA), the Pittsburgh Liver Research Center, Rho Chi Society and American Foundation for Pharmaceutical Education (USA), and the University of Pittsburgh School of Pharmacy (USA).

Author contributions

Gundala Venkata Naveen Kumar, Wen Xie, and Christian A. Fernandez conceptualized the research. Gundala Venkata Naveen Kumar, Keito Hoshitsuki, Sanjay Rathod, and Manda J. Ramsey performed the experiments. Gundala Venkata Naveen Kumar, Keito Hoshitsuki, Lauren Kokai, Erin E. Kershaw, Wen Xie, and Christian A. Fernandez analyzed the data. Gundala Venkata Naveen Kumar, Keito Hoshitsuki, and Christian A. Fernandez prepared the manuscript. All authors have approved the final article.

Conflicts of interest

The authors declare no conflicts of interest.

Appendix A. Supporting information

Supporting data to this article can be found online at https://doi.org/10.1016/j.apsb.2021.11.022.

References

1. Nakamura A, Nambu T, Ebara S, Hasegawa Y, Toyoshima K, Tsuchiya Y, et al. Inhibition of GCN2 sensitizes ASNS-low cancer cells to asparaginase by disrupting the amino acid response. *Proc Natl Acad Sci U S A* 2018;**115**:E7776–85.
2. Chen SH. Asparaginase therapy in pediatric acute lymphoblastic leukemia: a focus on the mode of drug resistance. *Pediatr Neonatol* 2015;**56**:287–93.
3. Stock W, Douer D, DeAngelo DJ, Arellano M, Advani A, Damon L, et al. Prevention and management of asparaginase/pegasparaginase-associated toxicities in adults and older adolescents: recommendations of an expert panel. *Leuk Lymphoma* 2011;**52**:2237–53.
4. Sallan SE. Myths and lessons from the adult/pediatric interface in acute lymphoblastic leukemia. *Hematology Am Soc Hematol Educ Program* 2006;**1**:128–32.
5. Stock W, La M, Sanford B, Bloomfield CD, Vardiman JW, Gaynon P, et al. What determines the outcomes for adolescents and young adults with acute lymphoblastic leukemia treated on cooperative group protocols? A comparison of Children's Cancer Group and Cancer and Leukemia Group B studies. *Blood* 2008;**112**:1646–54.
6. Boissel N, Auclerc MF, Lheritier V, Perel Y, Thomas X, Leblanc T, et al. Should adolescents with acute lymphoblastic leukemia be treated as old children or young adults? Comparison of the French FRALLE-93 and LALA-94 trials. *J Clin Oncol* 2003;**21**:774–80.
7. de Bont JM, Holt B, Dekker AW, van der Does-van den Berg A, Sonneveld P, Pieters R. Significant difference in outcome for adolescents with acute lymphoblastic leukemia treated on pediatric *vs* adult protocols in The Netherlands. *Leukemia* 2004;**18**:2032–5.
8. Ramanujachar R, Richards S, Hann I, Webb D. Adolescents with acute lymphoblastic leukaemia: emerging from the shadow of paediatric and adult treatment protocols. *Pediatr Blood Cancer* 2006;**47**:748–56.
9. Testi AM, Valsecchi MG, Conter V, Vignetti M, Paoloni F, Giona F, et al. Difference in outcome of adolescents with acute lymphoblastic leukemia (ALL) enrolled in pediatric (AIEOP) and adult (GIMEMA) protocols. *Blood* 2004;**104**:1954.
10. Oettgen HF, Stephenson PA, Schwartz MK, Leeper RD, Tallai L, Tan CC, et al. Toxicity of *E. coli* L-asparaginase in man. *Cancer* 1970;**25**:253–78.
11. Cairo MS. Adverse reactions of L-asparaginase. *Am J Pediatr Hematol Oncol* 1982;**4**:335–9.
12. Parsons SK, Skapek SX, Neufeld EJ, Kuhlman C, Young ML, Donnelly M, et al. Asparaginase-associated lipid abnormalities in children with acute lymphoblastic leukemia. *Blood* 1997;**89**:1886–95.

13. Haskell CM, Canellos GP, Leventhal BG, Carbone PP, Serpick AA, Hansen HH. L-Asparaginase toxicity. *Cancer Res* 1969;**29**:974−5.
14. Whitecar Jr JP, Bodey GP, Harris JE, Freireich EJ. L-Asparaginase. *N Engl J Med* 1970;**282**:732−4.
15. Christ TN, Stock W, Knoebel RW. Incidence of asparaginase-related hepatotoxicity, pancreatitis, and thrombotic events in adults with acute lymphoblastic leukemia treated with a pediatric-inspired regimen. *J Oncol Pharm Pract* 2018;**24**:299−308.
16. Wetzler M, Sanford BL, Kurtzberg J, DeOliveira D, Frankel SR, Powell BL, et al. Effective asparagine depletion with pegylated asparaginase results in improved outcomes in adult acute lymphoblastic leukemia: cancer and Leukemia Group B Study 9511. *Blood* 2007;**109**:4164−7.
17. Pratt CB, Johnson WW. Duration and severity of fatty metamorphosis of the liver following L-asparaginase therapy. *Cancer* 1971;**28**:361−4.
18. Durden DL, Salazar AM, Distasio JA. Kinetic analysis of hepatotoxicity associated with antineoplastic asparaginases. *Cancer Res* 1983; **43**:1602−5.
19. Wilson GJ, Bunpo P, Cundiff JK, Wek RC, Anthony TG. The eukaryotic initiation factor 2 kinase GCN2 protects against hepatotoxicity during asparaginase treatment. *Am J Physiol Endocrinol Metab* 2013;**305**:E1124−33.
20. Nikonorova IA, Al-Baghdadi RJT, Mirek ET, Wang Y, Goudie MP, Wetstein BB, et al. Obesity challenges the hepatoprotective function of the integrated stress response to asparaginase exposure in mice. *J Biol Chem* 2017;**292**:6786−98.
21. Wilson GJ, Lennox BA, She P, Mirek ET, Al Baghdadi RJ, Fusakio ME, et al. GCN2 is required to increase fibroblast growth factor 21 and maintain hepatic triglyceride homeostasis during asparaginase treatment. *Am J Physiol Endocrinol Metab* 2015;**308**:E283−93.
22. Liu Y, Janke LJ, Li L, Relling MV. L-Carnitine does not ameliorate asparaginase-associated hepatotoxicity in a C57BL6 mouse model. *Leuk Lymphoma* 2019;**60**:2088−90.
23. Lu G, Karur V, Herrington JD, Walker MG. Successful treatment of pegaspargase-induced acute hepatotoxicity with vitamin B complex and L-carnitine. *Proc (Bayl Univ Med Cent)* 2016;**29**:46−7.
24. Al-Nawakil C, Willems L, Mauprivez C, Laffy B, Benm'rad M, Tamburini J, et al. Successful treatment of L-asparaginase-induced severe acute hepatotoxicity using mitochondrial cofactors. *Leuk Lymphoma* 2014;**55**:1670−4.
25. Gundala NKV, Das UN. Arachidonic acid-rich ARASCO oil has anti-inflammatory and antidiabetic actions against streptozotocin+high fat diet induced diabetes mellitus in Wistar rats. *Nutrition* 2019;**66**: 203−18.
26. Raju J, Bird RP. Alleviation of hepatic steatosis accompanied by modulation of plasma and liver TNF-alpha levels by *Trigonella foenum graecum* (Fenugreek) seeds in Zucker obese (*fa/fa*) rats. *Int J Obes (Lond)* 2006;**30**:1298−307.
27. Bi Y, Jiang M, Guo W, Guan X, Xu M, Ren S, et al. Sex-dimorphic and sex hormone-dependent role of steroid sulfatase in adipose inflammation and energy homeostasis. *Endocrinology* 2018;**159**: 3365−77.
28. Wada T, Ihunnah CA, Gao J, Chai X, Zeng S, Philips BJ, et al. Estrogen sulfotransferase inhibits adipocyte differentiation. *Mol Endocrinol* 2011;**25**:1612−23.
29. Sanchez M, Lin Y, Yang CC, McQuary P, Rosa Campos A, Aza Blanc P, et al. Cross talk between eIF2alpha and eEF2 phosphorylation pathways optimizes translational arrest in response to oxidative stress. *iScience* 2019;**20**:466−80.
30. Rizzari C, Lanvers-Kaminsky C, Valsecchi MG, Ballerini A, Matteo C, Gerss J, et al. Asparagine levels in the cerebrospinal fluid of children with acute lymphoblastic leukemia treated with pegylated-asparaginase in the induction phase of the AIEOP-BFM ALL 2009 study. *Haematologica* 2019;**104**:1812−21.
31. Kamal N, Koh C, Samala N, Fontana RJ, Stolz A, Durazo F, et al. Asparaginase-induced hepatotoxicity: rapid development of cholestasis and hepatic steatosis. *Hepatol Int* 2019;**13**:641−8.
32. Rakhshandehroo M, Knoch B, Muller M, Kersten S. Peroxisome proliferator-activated receptor alpha target genes. *PPAR Res* 2010; **2010**:612089.
33. Riccardi R, Holcenberg JS, Glaubiger DL, Wood JH, Poplack DG. L-Asparaginase pharmacokinetics and asparagine levels in cerebrospinal fluid of rhesus monkeys and humans. *Cancer Res* 1981;**41**:4554−8.
34. Xu HE, Lambert MH, Montana VG, Parks DJ, Blanchard SG, Brown PJ, et al. Molecular recognition of fatty acids by peroxisome proliferator-activated receptors. *Mol Cell* 1999;**3**:397−403.
35. Bunpo P, Dudley A, Cundiff JK, Cavener DR, Wek RC, Anthony TG. GCN2 protein kinase is required to activate amino acid deprivation responses in mice treated with the anti-cancer agent L-asparaginase. *J Biol Chem* 2009;**284**:32742−9.
36. Gomez E, Powell ML, Bevington A, Herbert TP. A decrease in cellular energy status stimulates PERK-dependent eIF2alpha phosphorylation and regulates protein synthesis in pancreatic beta-cells. *Biochem J* 2008;**410**:485−93.
37. Harding HP, Zhang Y, Bertolotti A, Zeng H, Ron D. Perk is essential for translational regulation and cell survival during the unfolded protein response. *Mol Cell* 2000;**5**:897−904.
38. Galindo RJ, Yoon J, Devoe C, Myers AK. PEG-asparaginase induced severe hypertriglyceridemia. *Arch Endocrinol Metab* 2016;**60**:173−7.
39. Liu Y, Fernandez CA, Smith C, Yang W, Cheng C, Panetta JC, et al. Genome-wide study links PNPLA3 variant with elevated hepatic transaminase after acute lymphoblastic leukemia therapy. *Clin Pharmacol Ther* 2017;**102**:131−40.
40. Xiong X, Wang X, Lu Y, Wang E, Zhang Z, Yang J, et al. Hepatic steatosis exacerbated by endoplasmic reticulum stress-mediated downregulation of FXR in aging mice. *J Hepatol* 2014;**60**:847−54.
41. Kalavalapalli S, Bril F, Koelmel JP, Abdo K, Guingab J, Andrews P, et al. Pioglitazone improves hepatic mitochondrial function in a mouse model of nonalcoholic steatohepatitis. *Am J Physiol Endocrinol Metab* 2018;**315**:E163−73.
42. Pineda Torra I, Gervois P, Staels B. Peroxisome proliferator-activated receptor alpha in metabolic disease, inflammation, atherosclerosis and aging. *Curr Opin Lipidol* 1999;**10**:151−9.
43. Zhao L, Zou X, Feng Z, Luo C, Liu J, Li H, et al. Evidence for association of mitochondrial metabolism alteration with lipid accumulation in aging rats. *Exp Gerontol* 2014;**56**:3−12.
44. Martin GG, Atshaves BP, McIntosh AL, Payne HR, Mackie JT, Kier AB, et al. Liver fatty acid binding protein gene ablation enhances age-dependent weight gain in male mice. *Mol Cell Biochem* 2009;**324**: 101−15.
45. Ohnuma T, Holland JF, Freeman A, Sinks LF. Biochemical and pharmacological studies with asparaginase in man. *Cancer Res* 1970; **30**:2297−305.
46. Zimmermann R, Strauss JG, Haemmerle G, Schoiswohl G, Birner-Gruenberger R, Riederer M, et al. Fat mobilization in adipose tissue is promoted by adipose triglyceride lipase. *Science* 2004;**306**:1383−6.
47. Cheng Y, Meng Q, Wang C, Li H, Huang Z, Chen S, et al. Leucine deprivation decreases fat mass by stimulation of lipolysis in white adipose tissue and upregulation of uncoupling protein 1 (UCP1) in brown adipose tissue. *Diabetes* 2010;**59**:17−25.
48. Du Y, Meng Q, Zhang Q, Guo F. Isoleucine or valine deprivation stimulates fat loss *via* increasing energy expenditure and regulating lipid metabolism in WAT. *Amino Acids* 2012;**43**:725−34.
49. Saito T, Wei Y, Wen L, Srinivasan C, Wolthers BO, Tsai CY, et al. Impact of acute lymphoblastic leukemia induction therapy: findings from metabolomics on non-fasted plasma samples from a biorepository. *Metabolomics* 2021;**17**:64.
50. Patel B, Kirkwood AA, Dey A, Marks DI, McMillan AK, Menne TF, et al. Pegylated-asparaginase during induction therapy for adult acute lymphoblastic leukaemia: toxicity data from the UKALL14 trial. *Leukemia* 2017;**31**:58−64.
51. Nikonorova IA, Zhu Q, Signore CC, Mirek ET, Jonsson WO, Kong B, et al. Age modulates liver responses to asparaginase-induced amino acid stress in mice. *J Biol Chem* 2019;**294**:13864−75.

52. Montgomery MK, Hallahan NL, Brown SH, Liu M, Mitchell TW, Cooney GJ, et al. Mouse strain-dependent variation in obesity and glucose homeostasis in response to high-fat feeding. *Diabetologia* 2013;**56**:1129−39.
53. Boden G, Shulman GI. Free fatty acids in obesity and type 2 diabetes: defining their role in the development of insulin resistance and beta-cell dysfunction. *Eur J Clin Invest* 2002;**32**(Suppl 3):14−23.
54. Woo Baidal JA, Lavine JE. The intersection of nonalcoholic fatty liver disease and obesity. *Sci Transl Med* 2016;**8**:323rv1.
55. Reinert RB, Oberle LM, Wek SA, Bunpo P, Wang XP, Mileva I, et al. Role of glutamine depletion in directing tissue-specific nutrient stress responses to L-asparaginase. *J Biol Chem* 2006;**281**:31222−33.
56. Xu C, He J, Jiang H, Zu L, Zhai W, Pu S, et al. Direct effect of glucocorticoids on lipolysis in adipocytes. *Mol Endocrinol* 2009;**23**:1161−70.